

Development of an electromechanical principle for wet and dry milling

Bernd Halbedel and Oleg Kazak

Department of Mechanical Engineering, Group for Inorganic-Nonmetallic Materials, Technische Universität Ilmenau, Gustav-Kirchhoff-Straße 6, D-98684 Ilmenau, Germany

E-mail: bernd.halbedel@tu-ilmenau.de

Abstract. The paper presents a novel electromechanical principle for wet and dry milling of different materials, in which the milling beads are moved under a time- and local-variable magnetic field. A possibility to optimize the milling process in such a milling machine by simulation of the vector gradient distribution of the electromagnetic field in the process room is presented. The mathematical model and simulation methods based on standard software packages are worked out. The results of numerical simulations and experimental measurements of the electromagnetic field in the working chamber of a developed and manufactured laboratory plant correlate well with each other. Using the obtained operating parameters, dry milling experiments with crushed cement clinker and wet milling experiments of organic agents in the laboratory plant are performed and the results are discussed here.

1. Introduction

Milling is an important but complicated and energy consuming process in the production of materials. The interest in improvement of milling processes in numerous industrial applications such as finest milling of pharmaceutical organic agents [1], raw materials for ceramics, material for building industries [2] as well the recycling [3] has increased steadily. The novel electromechanical principle can be a solution for improvement of milling in numerous applications, but still need methods and tools for the design and optimization of the milling machine.

A laboratory plant that we have developed and manufactured previously has shown very good milling results [4]. Furthermore, the power consumption is very low as a result of direct power supplying to the grinding media. The biggest energy fraction, around 74 % of the total power supplied to the machine, is going to the milling process itself and only 23 % to ohmic losses as well as 3 % to iron losses in the exciter systems [4].

The main running parameter of such a machine for milling (a so-called EMZ plant) is the magnetic flux density and the resulting electromagnetic force distribution in the process room. For future development of this principle and design of new machines it is very important to develop a suitable model for numerical simulation of the resulting electromagnetic force distribution and its optimization. The model for numerical simulation is developed based on ANSYS Maxwell. The convergence of the calculation mesh is tested with different software setup as well as with different applied currents and current frequencies. Simulations are carried out in 2D and 3D. Verification is done by comparing results in ANSYS Maxwell with COMSOL Multiphysics as well with experimental measurements of the electromagnetic field in the process room of the laboratory EMZ installation. Dry milling experiments of crushing cement clinker and wet milling experiments of organic agents in the laboratory plant are



executed using the obtained operating parameters. The results of these milling experiments are discussed.

2. Electromechanical milling principle (EMZ)

The electromechanical milling principle is based on the moving of hard magnetic milling beads under the influence of the electromagnetic force $\vec{F}_{\nabla B}$ generated by interaction between the vector gradient $\nabla \vec{B}$ of the magnetic field \vec{B} and the fixed magnetization \vec{M} of the milling beads as shown in Figure 1.

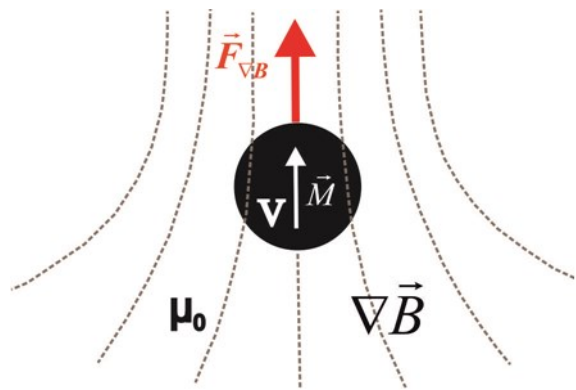


Figure 1. Magnetic force $\vec{F}_{\nabla B}$ on a milling bead with a magnetization \vec{M} and the volume V in a magnetic field \vec{B} with a vector gradient $\nabla \vec{B}$.

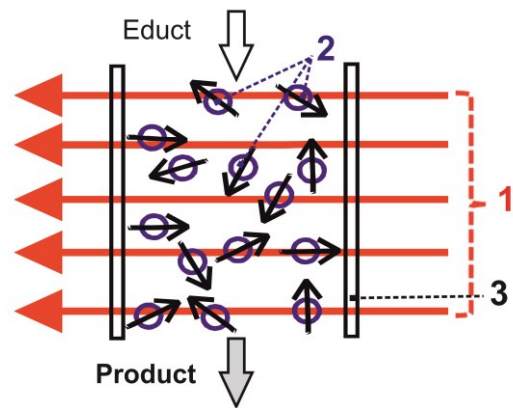


Figure 2. Principle of electromechanical milling (EMZ)
1 – time- and local-variable magnet field, 2 – hard magnetic milling beads, 3 – process room.

The generated force of one milling bead is given by equation (1):

$$\vec{F}_{\nabla B} = (\vec{p}_M \cdot \nabla) \vec{B}, \quad (1)$$

where \vec{p}_M is the vector of the magnetic moment, given for milling beads by

$$\vec{p}_M = \int_V \vec{M} dV = \frac{1}{\mu_0} \int_V \vec{J} dV, \quad (2)$$

with \vec{M} – the fixed permanent magnetization of the milling beads, \vec{J} – its magnetic polarization, V – the volume of a milling bead and $\mu_0 = 4\pi \cdot 10^{-7}$ Vs/Am – the absolute permeability.

With the simplifying assumptions that the magnetization of the milling bead is $\vec{M} = M = \text{const.}$ in its volume and directed in the same direction as $\nabla \vec{B}$ we can deduce equation (3) for description of the electromagnetic force density $\vec{f}_{\nabla B}$ on one milling bead:

$$\vec{f}_{\nabla B} = \frac{\vec{F}_{\nabla B}}{V} = M \cdot (\nabla \vec{B}) = \frac{1}{\mu_0} \vec{J} \cdot (\nabla \vec{B}), \quad (3)$$

with M – magnitude of \vec{M} and J – magnitude of \vec{J} .

As revealed in equation (3) the vector gradient of the magnetic field $\nabla \vec{B}$ dictates the direction of the force density $\vec{f}_{\nabla B}$ and the product $\vec{J} \cdot (\nabla \vec{B})$ determines their magnitude.

Additionally, if the magnetic vector gradient is time- and local-dependent, then a time- and local-dependent force density distribution $\vec{f}_{\nabla B}(r, \varphi, z, t)$ is generated in the process room, consequently an intensive relative movements between several milling beads are induced with different types of me-

chanical stresses so that the novel electromechanical milling principle can be used for disintegration of biomass, dry or wet grinding of raw materials and autogenously grinding of ferrites [4, 5].

The basic scheme of the electromechanical milling laboratory plant EMZ-LAI developed and manufactured previously by us is presented in Figure 2.

The process room is an annular gap bordered with non-ferromagnetic materials and surrounded internally and externally with a rotationally symmetrical exciter systems, which generate a rotating magnetic field $\vec{B}(r, \varphi, z, t)$. The designs of the exciter systems are analogical to an AC motor but with a large air gap between the outer (ESI) and the inner (ESII) exciter systems (cf. figure 3), which is used for milling.

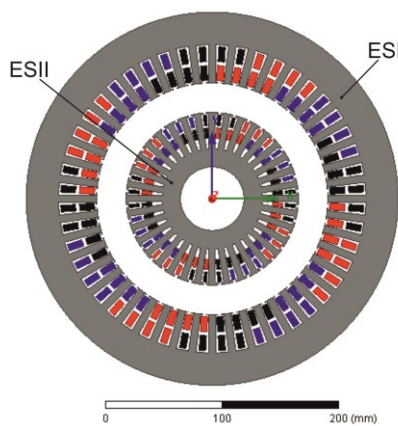


Figure 3. 2D cross section of the exciter systems ESI and ESII with the coils distribution, number of phases $m=3$, number of poles $2p=4$.

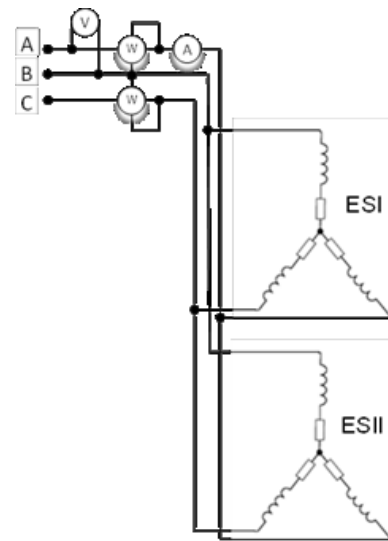


Figure 4. Electric connections of the windings from ESI and ESII to symmetric 3-phase system A, B and C with metering elements to measure the active power, voltage and current.

The windings of the exciter systems are performed with three phases and four poles. Figure 4 shows the electric connections of the windings from ESI and ESII to symmetric 3-phase system A, B, C.

3. Model for calculation of the electromagnetic design

The electromagnetic design of the EMZ machine is based on the consideration of equation (3) and the following important steps:

- determination of the required vector gradient $\nabla \vec{B}$ of magnetic field distribution $\vec{B}(r, \varphi, z, t)$ in the air gap with an existing EMZ plant and
- determination of a new design with the lowest possible losses at the required vector gradient $\nabla \vec{B}$.

For the determination of the vector gradient distribution $\nabla \vec{B}(r, \varphi, z, t)$, it is necessary to simulate the magnetic field distribution $\vec{B}(r, \varphi, z, t)$ in the air gap by equation (4)

$$\vec{B} = \text{rot} \vec{A} \quad \text{and} \quad \text{div} \vec{B} = 0, \quad (4)$$

where \vec{A} is the magnetic vector potential resulting from the design of the windings and electric current distribution in the exciter systems.

Then $\nabla \vec{B}(r, \varphi, z, t)$ is calculable using equation (5):

$$\nabla \vec{B} = \left(\frac{\partial B_r}{\partial r} + \frac{1}{r} \frac{\partial B_r}{\partial \varphi} + \frac{\partial B_r}{\partial z} - \frac{B_\varphi}{r} \right) \vec{e}_r + \left(\frac{\partial B_\varphi}{\partial r} + \frac{1}{r} \frac{\partial B_\varphi}{\partial \varphi} + \frac{\partial B_\varphi}{\partial z} + \frac{B_r}{r} \right) \vec{e}_\varphi + \left(\frac{\partial B_z}{\partial r} + \frac{1}{r} \frac{\partial B_z}{\partial \varphi} + \frac{\partial B_z}{\partial z} \right) \vec{e}_z \quad (5)$$

The losses in the exciter systems of an EMZ plant are calculated as sum of core losses $P_{v,U}$ in its laminated cores and ohmic losses $P_{v,R}$ in the coils

$$P_v = P_{v,R} + P_{v,U} \quad (6)$$

with

$$P_{v,R} = \frac{1}{2\sigma} \int_{V_c} j^2 dV \quad (7)$$

where σ is the electrical conductivity of the coils, j is the current density distribution in the windings and V_c is the winding volume, and

$$P_{v,U} = \int_{V_{lc}} \left[K_h \cdot f \cdot \hat{B}^2 + K_c \cdot (f \cdot \hat{B})^2 + K_e \cdot (f \cdot \hat{B})^{1.5} \right] dV, \quad (8)$$

where f is the frequency of the electric currents in the coils of the windings, \hat{B} are the values of the peak magnetic flux density in the laminated cores of the exciter systems, V_{lc} is the volume of the laminated cores, K_h is the hysteresis loss coefficient, K_c is the eddy current loss coefficient and K_e is the excessive loss coefficient. These coefficients are known from the data of the iron sheets producer.

To build a model for simulation of the electromagnetic field in ANSYS Maxwell, it is necessary to include the design of the laminated cores and the coils distribution of the inner and outer systems of the EMZ plant.

Figure 3 shows an example of usable laminated cores and coils distribution as well as their electric connection (see figure 4). The main geometrical parameters are an outer diameter of 322 mm and an air gap width of 25.5 mm. The number of slots of the outer system is 48 and of the inner system 36.

Symmetrical time-dependent current distributions according to the phase connection are presented by the following equations (9):

$$i_A = \hat{I} \cos(\omega t), \quad i_B = \hat{I} \cos(\omega t - \frac{2\pi}{3}), \quad i_C = \hat{I} \cos(\omega t - \frac{4\pi}{3}), \quad (9)$$

where $i_{A,B,C}$ are the instantaneous values of electric currents in the phases A, B and C of the exciter system and \hat{I} their peak value.

The calculation domain was split into uneven element sizes:

- + parts in the exciter systems with a large gradient of electromagnetic parameters, here the sizes of the cells are very small and
- + in the outer space with a small gradient of electromagnetic parameters, here the size of elements increases.

The mesh convergence presented in [6] as dependency of the error from the finite element number results in a low error of only 1.78 % at an element number of 13258. This result is suitable for simulation and all further simulations are carried out with this number of elements.

4. Results of the numerical simulations

The simulations of electromagnetic parameters are implemented for the following typical magnetic field strengths in the air gap of $H_\delta = 50, 70$ and 100 kA/m with a frequency of the electric currents of $f = 50$ Hz.

To verify the obtained simulation results, the experimental measurement of magnetic flux density distribution in the middle of the air gap is carried out with the help of Hall Probe MNT-4E04-VH (Lake Shore) and Gauss meter 421 (Lake Shore). The results of these experimental measurements

were compared with simulation data for the azimuthal and radial components. The relative differences amount up to maximal 7 %. This difference comes from the influence of the real magnetic properties and the geometry of the iron sheets, also from the discretization of the coil distribution.

The differences of the magnetic flux density magnitude B_{mag} obtained in ANSYS Maxwell and COMSOL Multiphysics are approximately 3 %. The differences between results in 2D and 3D simulation in all parameter distributions in the middle cross section reach 2-3 %.

The results of all comparisons attest that the developed numerical model is possible to be carried out in 2D and applicable for the electromagnetic design of exciter systems for electromechanical mills.

Figure 5 presents the radial and azimuthal component of the vector gradient of the magnetic field in the air gap of the manufactured EMZ plant on three circles, which are located in the near inner exciter system (R1), in the middle of the air gap (R8) and close to the outer exciter system (R16) at $H_\delta = 70$ kA/m and $f = 50$ Hz.

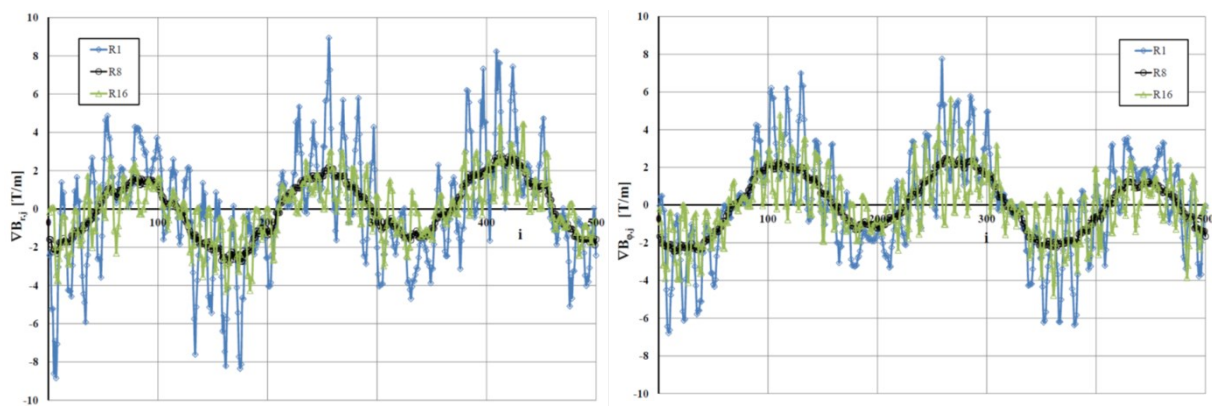


Figure 5. Radial $\nabla B_{r,j}(i)$ (left) and azimuthal $\nabla B_{\phi,j}(i)$ (right) components of the vector gradient of the magnetic field in the air gap of the manufactured EMZ plant on three circles j , which are located in the near inner exciter system (R1), in the middle (R8) of the air gap, and close to the outer exciter system (R16) dependent on i at $H_\delta = 70$ kA/m, $f = 50$ Hz, $\omega t = 0$.

The components of the vector gradient of the magnetic field have the same order up to 8 T/m, but their changes are larger close to the exciter systems (circle R1 and R16) than in the center of the air gap (R8). Consequently, the milling beads are more accelerated or braked close to the exciter systems. Here the movement changes are maximal.

In the center of the air gap the distribution is approximately sinusoidal along the circle R8. However, they are shifted, so that the azimuthal component $\nabla B_{\phi,j}$ is larger where the radial component $\nabla B_{r,j}$ is smaller or vice versa.

Other simulations [4] have shown that the magnitudes of the vector gradient components increase with the enhancement of the magnetic field strength H_δ in the air gap and the number of poles $2p$ as well as with the reduction of the number of slots per pole per phase ($q \rightarrow 1$) and of the chording of the windings ($\varepsilon \rightarrow 0$). These are the potentials for further improvements of the performance of mills based on the electromechanical principle [7].

5. Dry and wet milling in developed laboratory plant

To check this approach, experiments in the laboratory installation (EMZ-LAI) with crushed cement clinker (dry milling) and anthraquinone (wet milling) were performed in dependence on the magnetic field strength H_δ at constant current frequency f and fillings rates of the working chamber.

The specific energy consumption w_0 of EMZ-LAI dependent on the milling ratio z is presented in figure 6 in comparison with a ball mill (Bond) and a stirred ball mill (RWKM) and the same educt (cement clinker < 500 μm).

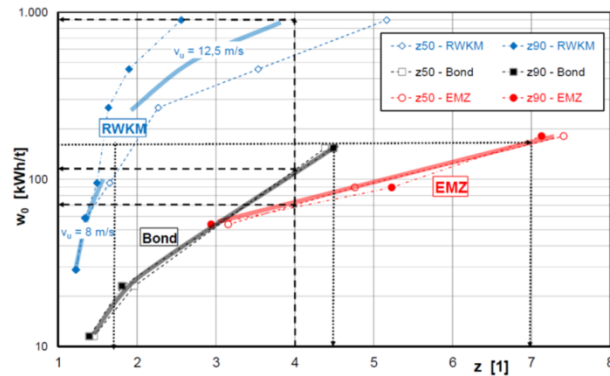


Figure 6. Specific energy consumption w_0 dependent on the milling ratio z of EMZ-LAI compared with a ball mill (Bond) and a stirred ball mill (RWKM with different stirrer speeds v_0) for dry milling of cement clinker < 500 μm .

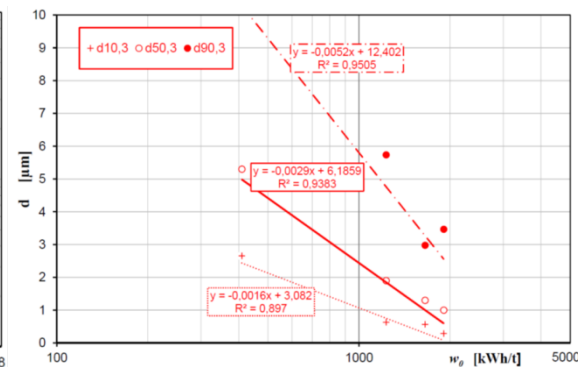


Figure 7. Particle sizes $d_{10,3}$, $d_{50,3}$, $d_{90,3}$ dependent on the specific energy consumption w_0 for wet milling of anthraquinone with input particle sizes of $d_{10,3} = 17.1 \mu\text{m}$, $d_{50,3} = 25.5 \mu\text{m}$ and $d_{90,3} = 37.1 \mu\text{m}$ in EMZ-LAI.

It is clearly derivable that the specific energy consumption of the EMZ-LAI is lower than w_0 of Bond and RWKM at the same milling ratio z (e.g. $z = 4$). The larger the required milling ratio of the product must be, the larger is the energetic advantage of EMZ principle. Furthermore, it is possible to achieve a high fineness (e.g. $z = 7$) only with the EMZ principle.

Figure 7 demonstrates the milling progress of a special aqueous model fluid which contains 5 wt-% anthraquinone particles (A90004-250G, Sigma-Aldrich Chemie GmbH / Taufkirchen) dependent on the specific energy consumption w_0 . The results of these experiments show that the anthraquinone particles are electromechanically grinded to $d_{50,3} < 1 \mu\text{m}$. However, the grinding progress for large particles ($d_{90,3}$; $d_{50,3}$) is faster than for small particles ($d_{10,3}$). The reason is the used size of the milling beads in the range of 1.0-1.6 mm. The implementation of larger grinding progress also for smaller particle sizes requires smaller milling beads < 1 mm.

6. Summary

Methods and approaches for numerical simulation of magnetic field and its vector gradient in ANSYS Maxwell and COMSOL Multiphysics are worked out. With the developed electromagnetic simulation tools on the basis of evaluation of the vector gradient distribution in the process room an up- and downscaling of EMZ plants is possible.

Furthermore, the possibility to confirm simulation results by experimental measurements and experimental milling results in the laboratory plant EMZ-LAI is shown.

The energy advantages for dry milling of building materials and wet milling of organic agents are shown using the example of cement clinker and using the example anthraquinone.

The next steps are the connection of the developed electromagnetic model with DEM-simulations [8] and with a stress model [9] to determine the required magnet field structure in the air gap for an efficient milling process.

References

- [1] Merisko-Liversidge E M and Liversidge G G 2008 Drug Nanoparticles: Formulating Poorly Water-Soluble Compounds. *Toxicologic Pathology* **36** 43-48 DOI: 10.1177/0192623307310946
- [2] Schäfer St and Hoenig V 2015 Chancen und Grenzen der energetischen Optimierung und CO₂-Reduktion in der Zementindustrie. 2. *Energiepanel Energieeffizienz und CO₂-Reduktion in der Industrie* Mainz 25.03.2015
- [3] Macko M Size 2012 Size Reduction by Grinding as an Important Stage in Recycling, *In: Post-Consumer Waste Recycling and Optimal Production* Edited by Enri Damanhuri Chapter **12** 273 - 294 DOI: 10.5772/2642
- [4] Halbedel B and Kazak O 2017 Potenziale eines neuen Mahlverfahrens – die elektromechanische Zerkleinerung (EMZ) *In „Produktgestaltung in der Partikeltechnologie* Bd. 8 FRAUN HOFER Verlag Stuttgart 181-196
- [5] Halbedel B, Ziolkowski M and Brauer H 2011 Potenziale des Elektromechanischen Zerkleinerungsprinzips. *In Proceedings: Workshop Elektroprozessstechnik*, Technische Universität Ilmenau, Ilmenau/Ortsteil Heyda 06.- 07. Oktober 2011 11
- [6] Kazak O and Halbedel B 2015 Approaches for modelling electromagnetic parameters in milling demonstration plant of organic agents *In: Proceedings 8th International Conference Electromagnetic Processing of Materials* Cannes / France 12-16 October 2015 4
- [7] Halbedel B and Kazak O 2017 Erregersystem für elektromechanische Mahlaggregate zum Zerkleinern, Desagglomerieren, Dispergieren und Mischen von dispersen Stoffen und pumpfähigen Mehrphasengemischen. DE 10 2017 008 513.7 23
- [8] <https://www.cfdem.com/liggghts-open-source-discrete-element-method-particle-simulation-code>, 26.10.2017
- [9] Kwade A and Stressing A 2003 A Stressing Model for the Description and Optimization of Grinding Processes. *Chemical Engineering & Technology* **26** (2) 199 – 205 DOI: 10.1002/ceat.200390029

Acknowledgment

The authors acknowledge financial support by the German Research Foundation (DFG) (Ha 2338/1) and by the Federal Ministry for Economic Affairs and Energy (BMWi) in ZIM-Cooperation Project EMZ-W (KF2184744KO4) as well as support by several industrial partners.